Micro-Raman Spectroscopy Study of Conjunctival Surface Epithelium in Dry-Eye Syndrome

Giulia Rusciano[1,2], Gianluigi Zito[1], Giuseppe Pesce[1], Antonio Sasso[1,2]

1 Department of Physics E. Pancini, University of Naples Federico II, via Cintia, 80126-I Naples, Italy.
2 Istituto Nazionale di Ottica (INO)-Consiglio Nazionale Delle Ricerche (CNR), Comprensorio "A. Olivetti," Via Campi Flegrei, Pozzuoli, Napoli 34-80078, Italy.

**giulia.rusciano@unina.it*

Keywords: micro-Raman spectroscopy; Dry-Eye Syndrome (DES); conjunctival surface epithelium.

Abstract

Dry eye syndrome (DES), also known as keratoconjunctivitis sicca, is a multifactorial disease of the ocular surface that results in ocular discomfort and a potential visual disturbance. From a microscopic point of view, DES can be related to an alteration of the structure of microvilli, cellular membrane protrusions on apical epithelial cells, which increase the surface area available for tear adherence. The aim of this study is to investigate the biochemical differences of conjunctival tissues from healthy donors and those from patients affected by DES using a confocal Raman system. Samples were obtained by impression cytology, a minimally invasive procedure to remove few superficial layers of the ocular surface epithelium. Our experimental outcomes demonstrate that the ratio between proteinaceous and lipidic Raman bands in conjunctival tissues from diseased donors is significantly altered with respect to healthy donors. The present study demonstrates that Raman spectroscopy can be potentially applied for an effective, non-invasive and potentially also in-vivo analysis of DES.

1. Introduction

Keratoconjunctivitis sicca, also called dry eye syndrome (DES) or keratitis sicca, is the most common eye disease, affecting 5-6% of the population [1-3]. It is a multifactorial disease, associated with a decreased tear production and/or increased tear film evaporation, which can have a high impact on the quality of life of afflicted individuals. Generally, DES leads only to mild irritation with no long-term effects. However, if left untreated, it can be a cause of visual disability or, in rare case, can lead to the loss of vision. Importantly, DES may compromise results of corneal, cataract, and refractive surgery. Dry eyes may also be prone to infections by pathogens (bacteria, prothozoa, yeasts) so that eye surface may become inflamed, causing scarring on the cornea [4].

A variety of treatment approaches are used, ranging from the use of artificial tears (for mild cases), to the insertion of punctal plugs into one of the small openings of tear drainage ducts that are located in the inner corner of the upper and lower eyelids to help tears to remain on the surface of the eye as long as possible. The choice of the correct medical approach for DES should clearly benefit of a medical test leading to a quantitative evaluation of the diseased eye state. However, at the moment, no single test seems to be adequate for establishing DES evolution and improve the clinician's understanding of the patient's condition.

The most employed tests include tear break-up time, ocular surface fluorescein staining and Schirmer test [5].

Herein, we propose a new approach to evaluate DES state based on micro-Raman analysis of the ocular surface epithelium obtained by Impression Citology (IC) [6].

Raman-based techniques have recently emerged as a formidable tool to access to the biochemical composition of many bio-systems, and its evolution under the application of external stimuli [7,8]. These techniques exploit the unique vibrational structure of molecular bonds in the sample (chemical fingerprinting). Nowadays, Raman Spectroscopy (RS) is revealing itself as a formidable alternative to fluorescence, as demonstrated by the increasing number of applications in many fields of life sciences. Many studies have been successfully carried out on both in vitro and in vivo biological systems to address various biomedical issues, including the early detection of malignant transformations and the rapid identification of pathogenic microorganisms [9]. Intriguingly, many applications of RS are emerging as reliable diagnostic tools in ophthalmology [10,11].

Recently, we have demonstrated that micro-Raman spectroscopy is an effective technique for differentiating patients affected by DES at different stages [12]. In particular, we analyzed the top most layer of bioptic samples taken in the conjunctival region which, in the eye, is in contact with the lacrimal fluid. It turned out that DES stage can be correlated to the density of microvilli, cellular membrane protrusions which increase the effective surface area available for tear adherence.

Herein, we extended that investigation to the cellular layers just underneath the microvilli region. In particular, we explore the possibility to differentiate samples from donors affected by pathogenic infections.

Although the present investigation can be only seen as a proof-of-principle demonstration, the obtained results hold

promise for the development of clinical protocols for DES diagnosis and evaluation.

2. Materials and methods

2.1. Sample preparation

Conjunctival epithelium cells were collected from the ocular surface of donors by Impression Cytology, a reliable, minimally invasive technique to remove the superficial layers of the ocular surface epithelium. According to this procedure, a strip of cellulose acetate is compressed on the bulb upper-temporal conjunctival surface for 3-4 s, therefore the adhered tissue is transferred onto a glass coverslip by compressing the cellulose acetate strip on the glass slide for several seconds, finally pulling it away [6]. During this transfer process, some residual of the cellulose tape could remain in contact with the transferred cells.

For this study, we analysed 10 patients under glaucoma therapy at the Eye Department, University of Naples Federico II, between September 2014 and January 2015. Inclusion criteria were age ≥18 years and bilateral or unilateral primary open-angle glaucoma. Exclusion criteria included the use of contact lenses and a history or slit-lamp evidence of ocular surface disorders different from DES.

2.2. Experimental Set-up

Raman analysis was performed by using a commercial Raman system (WiTec, alpha 300), described in details in ref. [13]. Briefly, it consist in a confocal microscope endowed with a Raman probe at 532 nm, focused on the sample with a 60× dry objective (N.A. = 0.8). The back-scattered radiation was collected with the same objective lens and, after spectral filtering of the Rayleigh spectral contribution by using an edge filter, it was guided toward the spectrograph by a 50 μm core optical fibre, which assures the confocality of the system. Spectra were acquired over the spectral range from 200 cm^{-1} to 3800 cm^{-1} (1024 points), with an integration time of 10 s. The laser power impinging on the sample was limited to 500 μW to avoid photoinduced-effects.

2.3. Data Analysis

Raman spectra acquired in this work were analyzed by Principal Component Analysis (PCA), a well-established multivariate statistical tool for the analysis of large data sets [14]. The basic idea is to reduce the dimension of data by condensing the information of the initial possibly correlated variables into a smaller number of uncorrelated variables (principal components, PC), defined by a linear combination of the original ones. When applied to Raman analysis, PCA allows the visualization of all the analysed spectra as scores in a multidimensional space, with the scores representing similar spectra grouped together. In this work, PCA was based on a homemade MATLAB (The MathWorks, Inc.) algorithm, based on the princomp.m routine. Before PCA, Raman spectra were background corrected by removing a forth-order polynomial and eliminating spurious signals deriving from cosmic rays contributions. The obtained PCA scores were further processed by Cluster analysis (CA) [15] in order to clusterize the PC scores into a given number of groups according to their distance in the PC scores space. In this work, PCA was performed by using a homemade algorithm, based on the use of the cluster.m MATLAB function.

3. Results and Discussion

3.1. Spectra collection

Sample collected by IC usually consisted of 2-3 epithelial cells layers adhered to the cellulose acetate used to remove the corneal tissue. Once transferred on the glass coverslip, the deepest cellular layers were put in contact with the glass coverslip. Samples were analyzed by collecting Raman spectra by moving the laser focal plane along the z-axis, keeping fixed the x and y coordinates (spectral coring) starting from the glass coverslip plane up to 20 μm, with a step of 0.5 μm.

In order to optimize the spectra signal-to-noise ratio, the integration time was set at 10 s. Spectral corings were repeated 3 times for each bioptic sample.

For this study, we analysed bioptic tissues from three groups of donors:

- *Class a*: tissues from donors not affected by DES, exhibiting a microvilli density σ higher than $3/\mu m^2$ (as revealed by Scanning Electron Microscopy); sample size:4.
- *Class b:* tissues from DES patients exhibiting a significant reduction of the microvilli density ($\sigma<0.1/\mu m^2$) with injuries present on the tissues; sample size:4.
- *Class c:* tissues from DES-affected patients ($\sigma<0.2/\mu m^2$) also exhibiting pathogenic infections; sample size:2.

Figure 1 reports the wide-field optical images of a bioptic sample of a DES-affected donor. From this image, it is possible to distinguish clearly the presence of cells, likely due to pathogens. However, optical images do not allow to distinguish between live and dead cells.

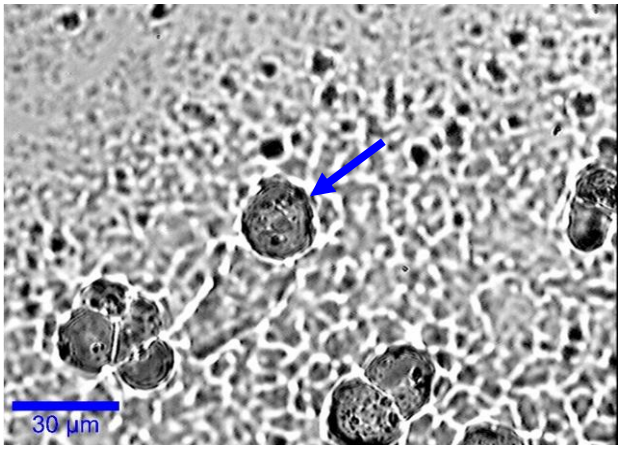

Fig. 1: Optical image of a tissue from *Class c*. The arrow highlight the presence of a pathogen.

Figure 2, instead, shows two Raman maps of the cell highlighted in Fig. 1 by the arrow. They were obtained by a x-

y scanning of the sample through the confocal Raman volume (step size: 0.5 μm). In particular, the left part of Fig. 2 reports the intensity of the peak the CH stretching band around 1440 cm^{-1} (mainly due to lipids) while the right image corresponds to the Amide I band around 1640 cm^{-1}, ascribed to proteins.

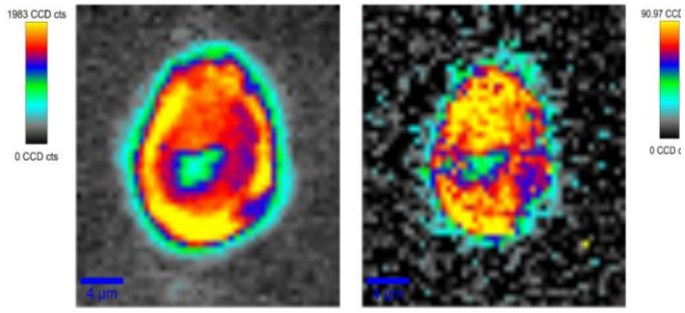

Fig. 2: Raman maps of the pathogen highlighted in Fig. 1 by the blue arrow. See text for details.

Notably, these Raman images highlight the presence of an intact membrane and a well-defined central nucleus, suggesting, therefore the presence of a living pathogen. This information that can be fundamental for clinicians for a correct treatment definition and a decision on its suspension.

3.2 Raman analysis

The first step of data analysis was aimed at selecting the spectra collected from the deeper cellular layers of the bioptic samples, therefore excluding the region containing microvilli. The details of the procedure followed at this purpose are reported in ref. [12].

Once identified the spectra corresponding to the deeper part of our bioptic samples, we averaged them, so that each bioptic sample was represented by the three spectra resulting from the three spectral corings performed on it. Finally, these spectra were analysed following the procedure described in the previous paragraph.

Figure 3 reports the classification dendrogram obtained as final output of this analysis. Labels 1-12, 13-24 and 25-30 correspond to *Class a*, *Class b* and *Class c* tissues, respectively. As it is possible to see, the spectra from donors affected by pathogenic infections are clearly differentiated by the other classes. This is not surprising. As a matter of facts, the presence of pathogens (or their dendris) can be revealed by Raman Spectroscopy, as demonstrated in ref. [16]. More interesting is the capability to differentiate normal and DES-affected donors. In particular, only one spectrum over twelve from *Class a* was misclassified by the grouping procedure.

Such a result, even if it does not present a complete separation between groups, are very promising, in consideration of the very low number of analysed samples. In order to get a deeper insight on such a discrimination capability, we considered the mean spectra for *Class a* and *Class b* analysed herein.

These spectra are shown in Fig. 4. Spectra were presented as row data. Some changes between the two classes appears, involving, in particular, the CH deformation band around 1440 cm^{-1} and the amide bands around 1640 cm^{-1} (Amide I) and 1260 (Amide III). In particular, the spectrum corresponding to *Class a* healthy donors clearly shows both lipid and proteniaceous bands. In more details, the sharp peak within the Amide III band at ~1282 cm^{-1} suggests the presence of proteins in α-helices conformation.

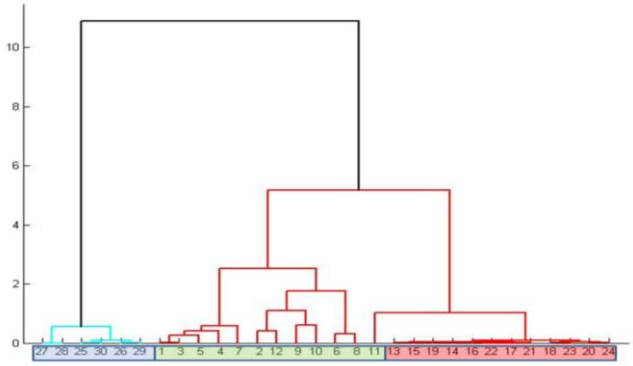

Fig. 3: Dendrogram showing the separation of Raman spectra from donors of the 3 different classes analysed in this work. Labels 1-12, 13-24 and 25-30 correspond to *Class a*, *b* and *c* tissues, respectively.

Conversely, the spectrum corresponding to the diseased donor (trace b), exhibits a reduced intensity of Amide bands. Moreover, the spectrum in trace b is dominated by the presence of features due to lipids, as the peaks at ~1450 cm^{-1}. The reason for this difference is still under investigation. However, it is reasonable to speculate that it could be related to the effect of an higher concentration of activated protease, such as matrix metallopeptidase (MMP-9), a molecule which leads to inflammation of cellular tissue [17]. Work is going on in our laboratory to shed light on this issue.

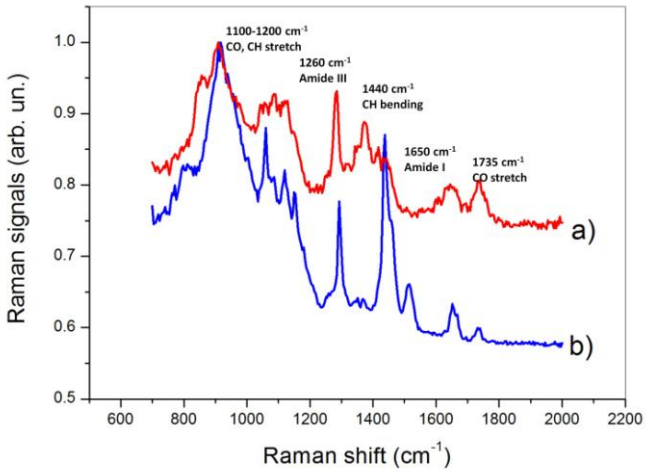

Fig. 4: Mean spectra for the three classes of samples analysed in this work.

4. Conclusions

In summary, the present work demonstrates that Raman Spectroscopy can represent a valuable tool to differentiate

patients affected by DES. Importantly, this technique sheds light on the biochemical difference of conjunctival tissues from healthy and DES-affected donors.
Further work is going on in our laboratory, concerning a much larger number of donors. A more detailed definition of groups, according to the observed microvilli density will be also considered.

Acknowledgements

GZ acknowledges a postdoctoral fellowship by Italian MIUR, grant number FIRB 2012- RBFR12WAPY.

References

[1] Davidson, H.J., Vanessa, J.K., 'Tear film and ocular mucins' Vet. Ophthalmol., 2004, 7, pp. 71-77.
[2] M. Meloni, B. De Servi, D. Marasco, and S. Del Prete, 'Molecular mechanism of ocular surface damage: Application to an in vitro dry eye model on human corneal epithelium', Mol. Vis., 2011, 17, pp.113-126.
[3] Perry, H.D. 'Dry eye disease: pathophysiology, classification, and diagnosis' Am. J. Manag. Care, 2008, 14, S79–87.
[4] Klotz, S.A., Penn, C.C., Negvesky, G. J., Butrus, S.I. 'Fungal and Parasitic Infections of the Eye' Clin Microbiol Rev., 2000, 13(4), pp. 662-685.
[5] Lin, H., Yiu, S.C. Saudi Journal of Ophthalmology, 2014, 28, pp. 173-181.
[6] Cennamo, G., Forte, R., Del Prete, S., Cardone, D., Cornea, 2013, 32, pp. 1227-1231.
[7] Rusciano, G., Zito, G. Isticato, R., Sirec, T., Ricca, E., Bailo, E., Sasso, 'Nanoscale chemical imaging of Bacillus subtilis spores by combining tip-enhanced Raman scattering and advanced statistical tools' A. ACS Nano, 2014, 8, pp. 12300-12309.
[8] Rusciano, G., De Luca, A.C., Pesce, G., Sasso, A. "On the interaction of nano-sized organic carbon particles with model lipid membranes", 2009, Carbon, 47 pp. 2950-2957.
[9] Isticato, R., Sirec, T., Giglio, R., Baccigalupi, L., Rusciano, G., Pesce, G., Zito, G., Sasso, A., De Felice, M., Ricca, E., Plos One, 2013, 8, pp. e74949.
[10] Erckens, R.J., Jongsma F.H.M., Wickstead, J.P., Hendrikse, F., March, W.F., Motamedi, M., 'Raman Spectroscopy in Ophthalmology: From Experimental Tool to Applications In Vivo' Lasers Med. Sci., 2001, 16, 236-252.
[11] Rusciano, G., Capriglione, P., Pesce, G., Del Prete, S., Cennamo, G., Di Cave, D., Cerulli, L., Sasso, A., Plos One, 2013, 8, e72127-1-8.
[12] Rusciano, G., Zito, G., Pesce, G., Del Prete, S., Cennamo, G., Sasso, A. 'Assessment of conjunctival microvilli abnormality by micro-Raman analysis', J. Biophot, 2016, 9(5), pp. 551-559.
[13] G. Zito, G, Rusciano, G. Pesce, A. Dochshanov, A. Sasso "Surface-enhanced Raman imaging of cell membrane by a highly homogeneous and isotropic silver nanostructure", 2015, Nanoscale, 7, pp. 8593-8606.
[14] Rusciano, G., 'Experimental analysis of Hb oxy–deoxy transition in single optically stretched red blood cells' Phys. Med., 2010, 26, pp. 233-239.
[15] Fraley, C., Raftery, A.E.,'Model-based clustering, discriminant analysis, and density estimation' Journal of the American Statistical Association, 2002, 97, pp. 611-631.
[16] Rusciano, G., Capriglione, P., Pesce, G., Abete, P., Carnovale, V., Sasso, A. 'Raman spectroscopy as a new tool for early detection of bacteria in patients with cystic fibrosis', Laser Phys. Lett., 10, pp. 075603-1-13.
[17] Chotikavanich, S., de Paiva, C.S., Lee, D.Q. 'Essential Role for c-Jun N-Terminal Kinase 2 in Corneal Epithelial Response to Desiccating Stress', Invest. Ophthalmol. Vis. Sci., 2009, 50, pp. 3203-3209.